



Original article

Influence of most reactive inorganic cation in the optical and biological activities of L-Lysine monohydrochloride crystal

B. Aneeba^{a,*}, S.V. Ashvin Santhia^a, S. Vinu^{b,*}, R. Sheela Christy^a, Dunia A. Al Farraj^c, Noorah A. Alkubaisi^c^a Department of Physics and Research Centre, Nesamony Memorial Christian College, Marthandam, Affiliated to Manonmaniam Sundaranar University, Abishekapatti, Tirunelveli, TamilNadu, India^b Department of Physics, Government Arts and Science College, Nagercoil, Tamil Nadu 629004, India^c Department of Botany and Microbiology, College of Science, King Saud University, Riyadh 11451, Saudi Arabia

ARTICLE INFO

Article history:

Received 18 May 2020

Revised 12 July 2020

Accepted 14 July 2020

Available online 18 July 2020

Keywords:

Slow evaporation

Semiorganic crystal

Potassium

Optical property

Conductivity

Pathogenic bacteria

ABSTRACT

Slow evaporation method was used to grow the pure and K⁺ ion doped L-Lysine monohydrochloride (L-LMHCL) crystals which has optical and antibiotic applications. The space group, structure and slight shifting of peaks are confirmed using single crystal XRD and the powder XRD. The FTIR analysis also shows that the K⁺ doped L-LMHCL has a slight shifting in the spectrum which indicates the functional group of L-LMHCL and the interaction between the K⁺ ions. The existence of K⁺ ion in the doped crystal is assured by the presence of potassium in the EDAX spectrum. The wide optical band gap was found for pure and K⁺ doped crystal using UV spectra and these are utilized in optoelectronic and nonlinear applications. The Kurtz Perry technique specified the NLO property of grown crystals. The dielectric property crystals was studied by varying the temperature. As a result, the highest dielectric constant is observed in doped crystal. An antibacterial activity against certain bacteria like E-coli, pseudomonas aeruginosa and staphylococcus aureus are provided by mm range for the grown crystals.

© 2020 The Author(s). Published by Elsevier B.V. on behalf of King Saud University. This is an open access article under the CC BY-NC-ND license (<http://creativecommons.org/licenses/by-nc-nd/4.0/>).

1. Introduction

Aminoacid based organic crystals are potential candidates for optical application as it possesses chiral carbon atom, proton acceptor (NH₂) known as zwitterions, non-centrosymmetric space groups and flexibility of molecular design (Shanmuga Sundaram et al., 2019) but it has poor physio-chemical stability and low mechanical strength (Min-hua jiang and Qi Fang., 1999). It can be prone to exhibit wide transparency range, mechanical strength, high polarizability, chemical stability, good second harmonic generation (SHG) and low angular sensitivity (Allen moses et al., 2019; Kandhan et al., 2019) when it combines with inorganic compounds known as semiorganic. Due to the enticing features of hybrid nonlinear optical (NLO) crystals, it is used in the field of data storage, optical communication, laser remote sensing, mode locking, night vision devices etc. (Kui et al., 2017; Kandhan et al., 2018). The novel transparent

electro- and elasto-optical material is L-Lysine monohydrochloride crystal (Ozga et al., 2008). It owns three reactive groups like α-carboxyl, α and ε-amino group also immunostimulatory effect on inoculation site infections (Zhang et al., 2020; Ayala and Krikorian, 1989). Since last decade slow evaporation solution growth was preferred by many researchers to grow defect free crystal due to its simplest and cost-effective method. The various reviews show that the impurities also make changes in the properties of molecules (Helen and Kanchana, 2014). For the first time, in order to enhance the optical, dielectric, nonlinear and antibacterial activities the most reactive potassium ion was introduced as dopant into the lattice of L-LMHCL via slow evaporation method. Obtained crystals are being characterized by using the methods such as Single crystal X-ray Diffraction (SXRD), powder XRD, Fourier Transform Infrared Spectroscopy (FTIR), Energy Dispersive X-ray Analysis (EDX), UV-Visible spectroscopy, Micro hardness, second order nonlinear optical studies, Dielectrics and Antibacterial studies.

* Corresponding authors.

E-mail addresses: aneebaanu@gmail.com (B. Aneeba), vinusnist@gmail.com (S. Vinu).

Peer review under responsibility of King Saud University.



Production and hosting by Elsevier

2. Materials and methods

2.1. Materials

The materials Lysine monohydrochloride and KCl used for this exploration were purchased from Sigma Aldrich Chemicals.

<https://doi.org/10.1016/j.sjbs.2020.07.018>

1319-562X/© 2020 The Author(s). Published by Elsevier B.V. on behalf of King Saud University.

This is an open access article under the CC BY-NC-ND license (<http://creativecommons.org/licenses/by-nc-nd/4.0/>).

2.2. Growth of undoped and doped L-Lysine monohydrochloride crystal

At constant temperature, pure and potassium added L-LMHCL crystals are grown using the conventional slow evaporation technique. The computed amount of L-Lysine monohydrochloride ($C_6H_{15}ClN_2O_2$) was dissolved in the deionized water. At 40 °C temperature, the solution was stirred continuously for about 2 hrs to make sure of homogenous supersaturated solution. To obtain K^+ ion doped L-LMHCL crystal, 1 mol% of potassium chloride (KCl) was added to the L-LMHCL solution. The solutions were filtered twice in a clean rinsed beaker using whatmann filter paper to remove impurities. A perforated thin polyethylene sheet was used to close the beaker optimally. At room temperature, it was placed undisturbed for slow evaporation. The better-quality crystals which are optically transparent had been harvested within 20 days. The photographs of pure and doped crystals are shown in Fig. 1.

2.3. Antibacterial test

The susceptibility action against the pathogenic bacteria were carried out by standard Kirby-Bauer test commonly called disc diffusion test (Shen et al., 2019, Zou et al., 2020). The inhibited range of disease causing bacteria was identified from the zone formed around the compound and the diameter zone was measured in mm range using transparent mm scale.

3. Results and discussion

3.1. Single crystal X-Ray diffraction (SXRD)

ENRAF NONIUS CAD4 X-ray diffractometer was used to collect the single crystal XRD of pure and doped L-LMHCL crystals. The collected lattice parameter values show that the grown crystals belong to monoclinic structure with space group $P2_1$ because lattice parameters a , b , c are different and two interfacial angles are equal to 90° and other is not. Non-centro symmetric nature also confirmed from space group which is a rudimentary condition for SHG applications. The obtained lattice parameters of crystals are well compliance with the reported values (Ramesh Babu et al., 2006). Slight difference in unit cell parameters are generally caused by the change of periodicity in lattice vibrations at high temperature, concentration of dopant, electronic and size effect (Deepa and Philominathan, 2017). Here the reduction in the lattice parameters of K^+ doped L-LMHCL crystal was due to the effect of dopant K^+ ion in the lattices of L-LMHCL crystals.

3.2. Powder X-Ray diffraction (XRD) analysis

X'Pert Pro - PAnalytic powder diffractometer was used for powder X-ray diffraction studies. The studies were carried out with $0.2^\circ/\text{sec}$ scan speed and CuK_α radiation of wavelength 1.5418 \AA . The powder X-ray diffraction pattern of undoped and doped L-LMHCL is given in Fig. 2a.

Scanty shift in the intensity of peak and FWHM is obtained in the Fig. 2b as a result of strain in the crystalline lattice. There is no additional phase recommended since K^+ ion does not affect the entire lattice of L-LMHCL, but there is minute lattice distortion.

3.3. Fourier Transform Infrared (FTIR) spectroscopic study

FTIR spectra is a unique fingerprint of molecule that elucidate the various functional groups exist in the grown crystals. The FTIR analysis of the grown crystals were recorded in the middle IR region ($400\text{--}4000 \text{ cm}^{-1}$) by Thermo Nicolet Avatar 370 spectrometer (Fig. 3). This range is the most remarkable range in the study of organic, inorganic and semi organic compound (Pasupathi and Philominathan, 2008; Balasubramanian et al., 2010; Ushasree et al., 1999). The FTIR vibrational spectra and its assignments of grown crystals agree well with the literature values (Vasudevan et al., 2010) (see Table 1).

The band observed at 3443 cm^{-1} is assigned as NH_3^+ asymmetric stretching vibrations. The absorption band at 1624 cm^{-1} and 1506 cm^{-1} are attributed to weak asymmetric NH_3^+ bending and strong symmetric NH_3^+ bending. CH_2 twisting acknowledged at 1348 cm^{-1} . The band observed at 1140 cm^{-1} is attributed to NH_2 and NH_3 rocking. The peak observed at 996 cm^{-1} is due to C-C stretching. O-H-O out-of-plane bending type of vibrations of hydrogen bonds observed at 861 cm^{-1} . The band imputed at 553 cm^{-1} is the result of COO^- wagging. Table 2 shows the functional group assignments of obtained crystals. The spectrum of K^+ doped L-LMHCL provide the similar features of pure L-LMHCL, although there is shifting exist for most of the band insinuate that there is wide range of interactions between the K^+ ions with the function group of L-LMHCL.

3.4. Energy Dispersive X-ray analysis (EDX)

EDX is the most positive way to recognize the presence of accompanied elements in the obtained crystal. Fig. 4 displays the accounted EDAX spectrum, which was taken to confirm the presence of potassium in the doped crystal. It distinctly indicates the presence of various elements such as oxygen, carbon, potassium and chloride in the K^+ ion doped crystal. The existence of k^+ ion

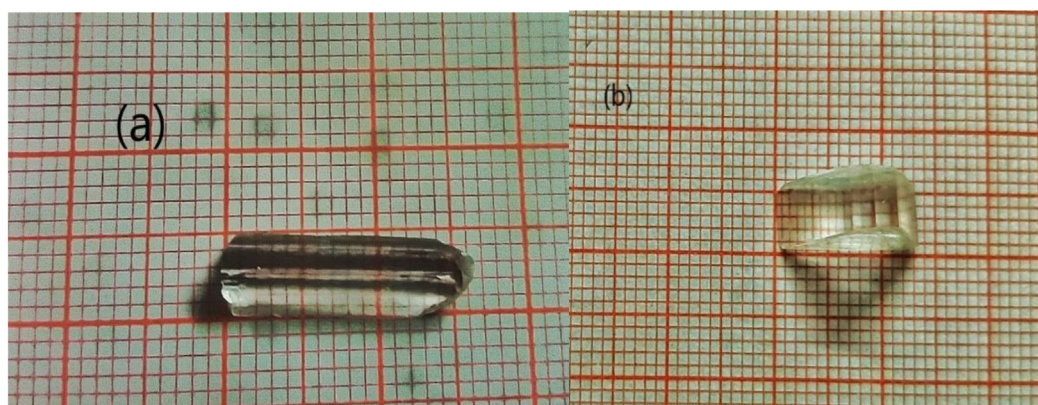


Fig. 1. Photograph of (a) pure L-LMHCL, (b) K^+ doped L-LMHCL crystals.

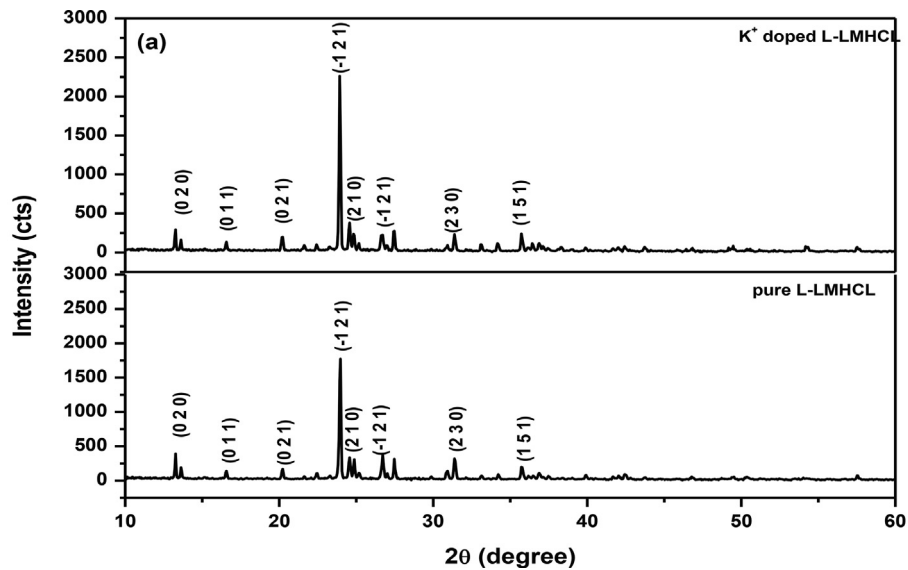


Fig. 2a. Powder XRD pattern of pure and K^+ doped L-LMHCL crystal.

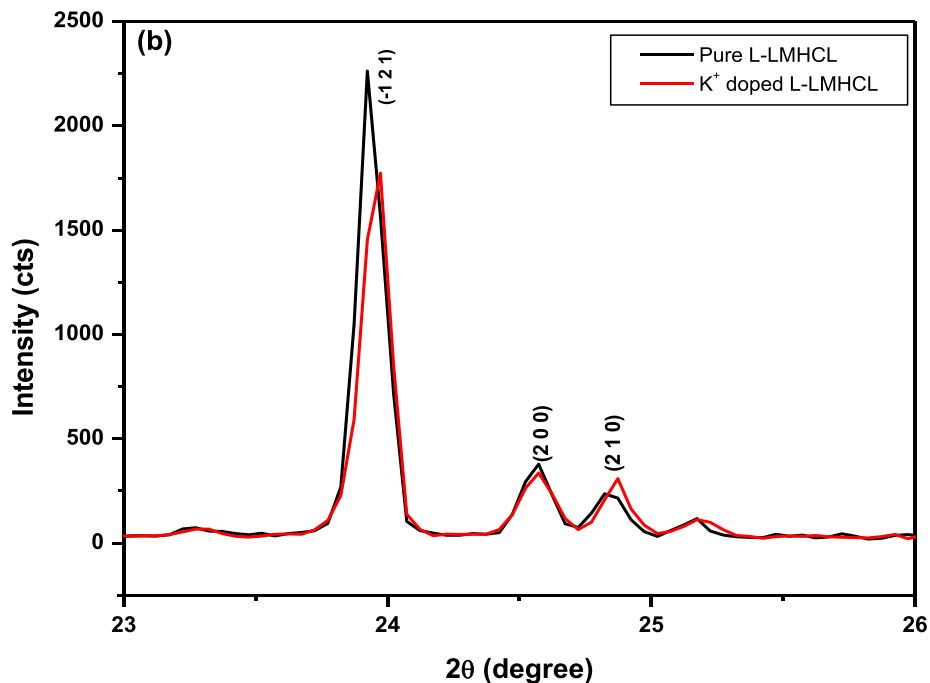


Fig. 2b. Peak shifting in pure and K^+ doped L-LMHCL.

in the doped crystal was confirmed by the trace of potassium in the EDAX spectrum.

3.5. Optical transmission spectral study

One of the important properties of crystal is its optical behaviour which mainly embraces the ultraviolet radiation which can either be absorbed or transmitted by the sample. The wide transparency nature of the crystal plays the main role in UV-tunable lasers, photonics and NLO device applications. In order to find the optical property, Perkin Elmer (Lambda 35) in the wavelength range of 198–800 nm was used. The polished crystal samples were subjected to be measured. The recorded transmittance spectrum of impure L-LMHCL crystal collated with undoped L-LMHCL crystal is

shown in Fig. 5(a). It indicates the presence of transmission in the whole UV-visible range. It is particularly seen in the second harmonic wavelength (532 nm) region, and also the transparency of K^+ ion doped L-LMHCL is slightly increased and cut-off wavelength shifted towards lower wavelength side because of the lack of grain and defect boundaries (Rathika and Ganapathi Raman, 2014). As the lower cut-off wavelength and optical transparency of good NLO material lies between 200 and 400 nm, the grown crystal can be considered as an NLO material (Kalaivani et al., 2015).

3.6. Measurement of optical band gap

The type of electronic transition and energy gap mainly depend on optical absorption coefficient and photon energy. The optical absorbance coefficient (α) is find out from the Eq. (1):

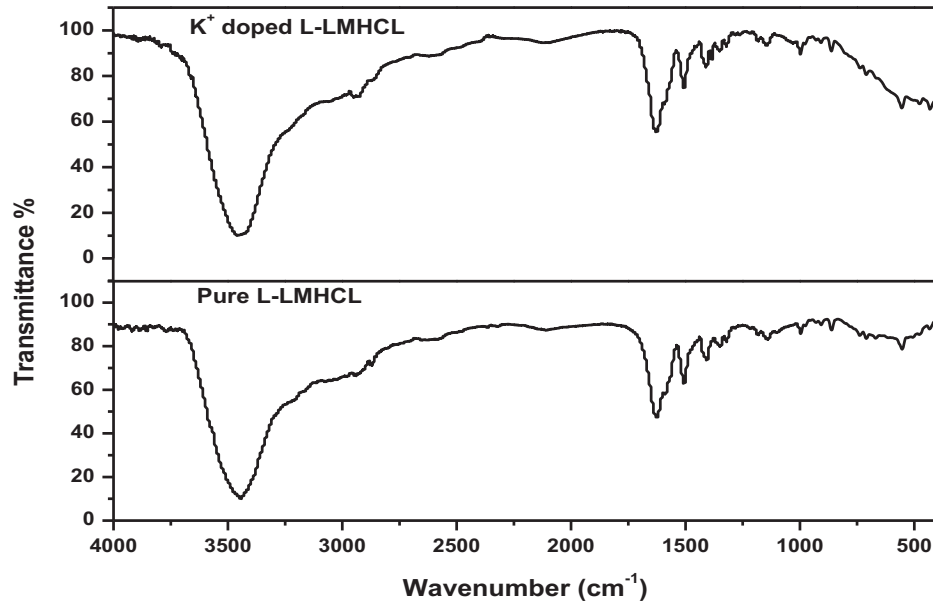


Fig. 3. FTIR spectra of pure and K⁺ doped L-LMHCL crystal.

Table 1
Unit cell parameters of pure and K⁺ doped L-LMHCL crystals.

Cell parameters	Pure L-LMHCL	K ⁺ doped L-LMHCL
a (Å)	5.92	5.88
b (Å)	13.39	13.35
c (Å)	7.54	7.50
α = γ	90°	90°
β	97.91°	97.81°
cell volume V (Å ³)	592	584

Table 2
FTIR vibrational band assignments of pure and K⁺ doped L-LMHCL crystal.

Wave number (cm ⁻¹)	Vibrational band assignments	
L-LMHCL	K ⁺ doped L-LMHCL	
3443	3457	NH ₃ ⁺ asymmetric stretching
-----	2114	Asymmetric NH ₃ ⁺ bending vibration
1624	1626	weak asymmetric NH ₃ ⁺ bending
1506	1506	strong symmetric NH ₃ ⁺ bending
1406	1408	COO ⁻ symmetric stretching
1348	1384	CH ₂ twisting
1140	1142	NH ₂ and NH ₃ Rocking
996	997	C—C stretching
861	861	O—H—O out-of- plane bending
553	554	COO— wagging

$$\alpha = \frac{2.303 \log(\frac{1}{T})}{d} \quad (1)$$

where 'T' and 'd' are transmittance and thickness of the crystal. Direct band gap was recommended from the energy dependence of absorption coefficient and hence for high photon energy it obeys Tauc's relation is given in Eq. (2): (Tauc, 1974).

$$\alpha h\nu = A(h\nu - E_g) \quad (2)$$

Fig. 5(b) illustrates the extrapolated graph between $(\alpha h\nu)^2$ and $h\nu$ owing to the direct allowed transition of crystals and the graph imputed the value of E_g . By the extrapolation of straight-line portion to $(\alpha h\nu)^2 = 0$, 5.52 eV for undoped and 5.89 eV for K⁺ doped

L-LMHCL crystals were founded, and this wideband gap values utilized in optoelectronic and nonlinear optical application. It also shows the ability of dielectric (crystal) medium to be polarized when external field is applied.

3.7. Nonlinear optical (NLO) study

Kurtz-perry powder technique was the important tool used to assess obtained crystal's second harmonic generation (SHG) (Kurtz and Perry, 1968). The green light (532 nm) emitted by the crystals when it was exposed to radiation from Nd: YAG laser of wavelength 1064 nm confirms the NLO nature of the crystals. When Compared to standard KDP crystal's SHG efficiency, the pure and doped crystal's SHG efficiency are 1.2 and 1.6 times greater. From the observation it is clear that the presence of K⁺ ion enhance the SHG efficiency of the L-LMHCL. This result strongly recommends that the harvested crystals are propitious for SHG implementation.

3.8. Dielectric analysis

The study of dielectric behaviour at different temperature with various frequencies of applied field gives important electrical properties of the materials like polarizability, phase change, nature of atoms and charge transport mechanism of the crystal (Karuppasamy et al., 2017). With the use of two probe set up, dielectric behaviour was measured. In the middle of the copper electrode which behaves as parallel plate capacitor double side graphite coated crystal was placed this double side graphite coated crystal act as dielectric material. By changing the temperature from 40 °C to 140 °C and frequency from 100 HZ to 1 MHZ corresponding capacitance values were noted. Dielectric constant (ϵ_r) was measured by the Eq. (3), Balaji et al. (2020)

$$\epsilon_r = \frac{ct}{\epsilon_0 A} \quad (\text{Balaji et al., 2020}) \quad (3)$$

Change in dielectric constant and dielectric loss ($\tan\delta$) with different temperature and applied frequency are shown in Fig. 6(a), (b), (c) and (d). All polarization namely, space charge, orientation, ionic and electronic polarization are present at low frequency as the result of high value of ϵ_r and $\tan\delta$. The decrease in ϵ_r and $\tan\delta$

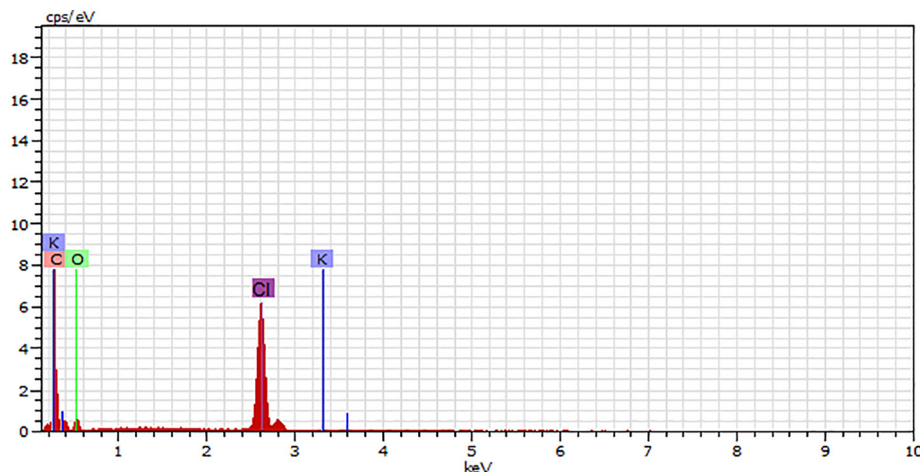


Fig. 4. EDAX spectra of K^+ doped L-LMHCL.

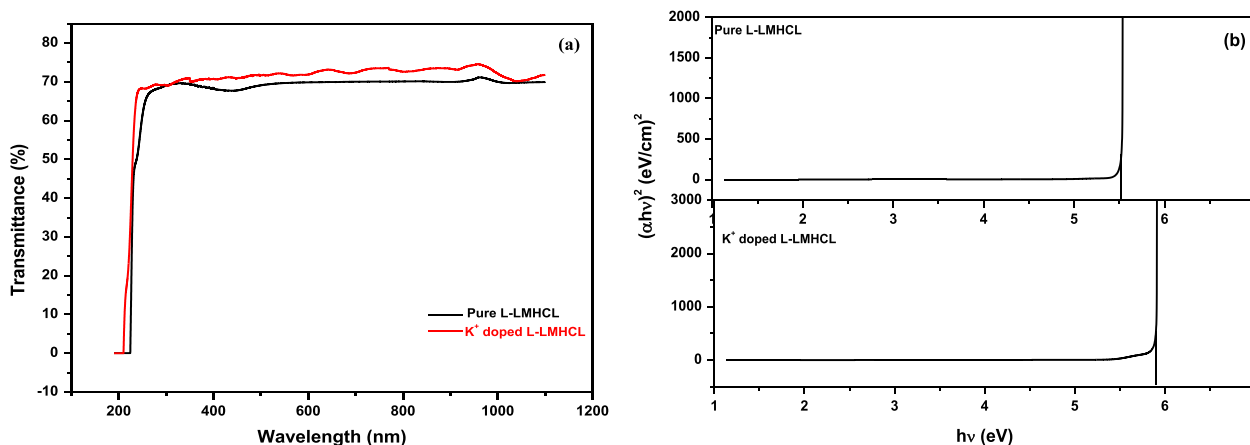


Fig. 5. (a) Transmission spectra of pure and K^+ doped L-LMHCL crystal and (b) Tauc's plot of pure and K^+ doped L-LMHCL crystals.

when the frequency increases suggest that these polarization diminishes gradually and electronic polarization only exist and indicate less detect (Sivavishnu et al., 2018). These attributes of the crystals are used in the photonics and NLO applications because polarizability depend on linear susceptibility, and linear susceptibility proportional to SHG (Raval et al., 2019). Further, correlating the magnitude of ϵ_r of K^+ mixed and unmixed L-LMHCL crystals reveals that potassium added crystals possess high ϵ_r and $\tan\delta$. High dielectric constant material exposes high polarizability due to mobility of dipoles, which type of materials are contribute high SHG efficiency. The change in conductivity at various temperature and angular frequency is shown in Fig. 6(e) and (f). The conductance of doped crystal is more than pure crystal. There is motion of charge carrier increases with temperature which lead to high value of conductivity.

3.9. Antibacterial activity

Antibacterial activities of pure and K^+ ion doped L-LMHCL crystals assessed quantitatively by most widely used antibiotic susceptibility test Kirby-Bauer method. The organism was susceptible by the sample and can be identified from the diameter of zone formation around the grown powdered crystal sample. Observed inhibition zone in the millimeter (mm) range, compared to the standard drug Amikacin is shown in Table 3, indicating that doped crystal showed good inhibitory action against pseudomonas aeruginosa

and staphylococcus aureus bacteria than pure crystal and the antibacterial activity of pure L-LMHCL crystal towards Escherichia coli is more than doped L-LMHCL crystal. Zone resisting action of crystals against *pseudomonas aeruginosa* is leading than HTNN crystal (Ravathi and Karthik, 2019) also it have more inhibitory action on *Staphylococcus aureus* than Ag nanoparticles. (Prakasha et al., 2013).

4. Conclusion

Single crystals of pure and k^+ doped L-LMHCL were grown by slow evaporation method. Monoclinic structure and the $P2_1$ space group nature of the obtained crystal was revealed when it undergoes X-ray diffraction analysis. The K^+ ion does not affect the entire lattice of L-LMHCL, identified from the single-phase nature of powder XRD. The existence of functional groups and elements were corroborate by FTIR and EDX analysis. The optical absorbance study reveals that the percentage of transmission was increased by adding K^+ ions. The obtained crystal's SHG efficiency were 1.2 and 1.6 times higher than that of KDP. Dielectric measurements of crystals were carried out and the results were discussed. The pure and doped L-LMHCL crystals show good inhibitory antibacterial property when exposed to bacteria. The above said studies confirmed that K^+ doped L-LMHCL crystals have enhanced properties than pure L-LMHCL crystals and could be treated as a promising material for fabricating the optoelectronic devices and antibiotics.

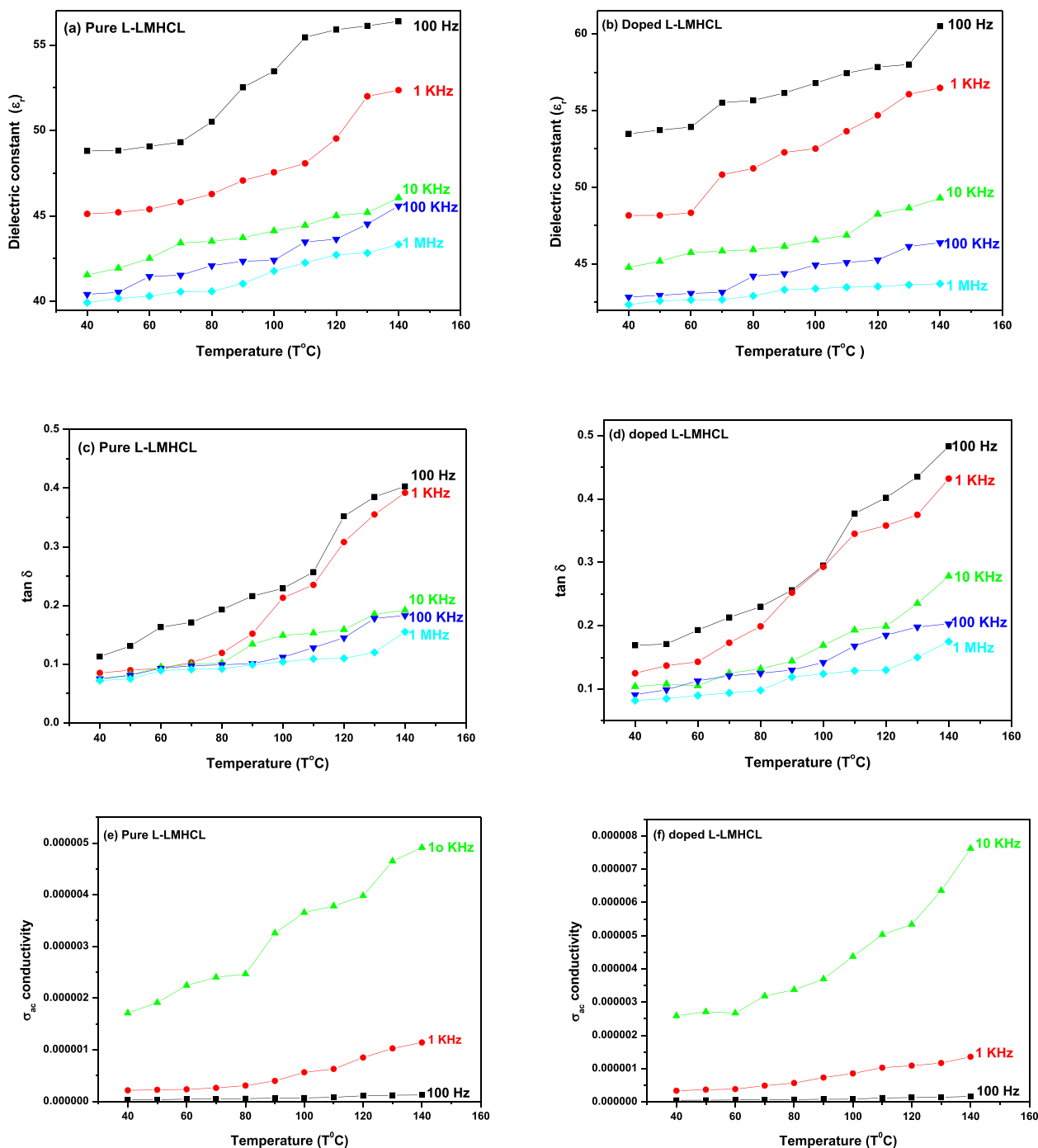
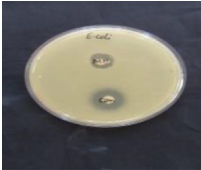

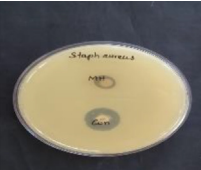
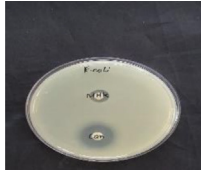
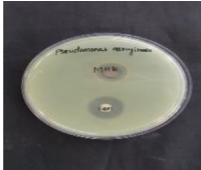



Fig. 6. Plot of ϵ_r versus temperature of (a) pure and (b) K^+ doped L-LMHCL crystal (c) $\tan \delta$ versus temperature of pure and (d) K^+ doped L-LMHCL crystal (e) Conductivity versus temperature of pure and (f) K^+ doped L-LMHCL crystal.

Table 3
Zone of inhibition of pure and doped crystals.

Pure L-LMHCL			K^+ doped L-LMHCL		
E.coli	Pseudomonas aeruginosa	Staph aureus	E.coli	Pseudomonas aeruginosa	Staph aureus
15 mm	16 mm	12 mm	13 mm	17 mm	13 mm
					

Acknowledgments

The authors are grateful to SAIF IIT, Chennai, STIC, Cochin, St. Joseph College, Tiruchirappalli, Consultancy on Characterization of Nanomaterials (CCN), The Gandhigram Rural Institute – Deemed University Gandhigram and Department of Physics, Alagappa University, Karaikudi for the facilities provided for various analysis. The authors extend their appreciation to the Researchers supporting project number (RSP-2020/190) King Saud University, Riyadh, Saudi Arabia.

Disclosure statement

No potential conflict of interest regarding the publication of this paper was reported by the authors.

References

- Allen Moses, S.E., Tamilselvan, S., Ravi Kumar, S.M., Johnson, J., 2019. Synthesis, growth and characterization of semi-organic nonlinear optical L-threonium sodium fluoride (LTSF) crystal for photonics applications. *Chin. J. Phys.* 58, 294–302.
- Ayala, E., Krikorian, D., 1989. Effect of L-Lysine monohydrochloride on cutaneous herpes simplex virus in the guinea pig. *J. Med. Virol.* 28, 16–20.
- Balaji, J., Srinivasan, P., Prabu, S., Merin George, Sajan, D., 2020. Growth and dielectric studies of toluidine tartrate single crystals: A novel organic NLO material. *J. Mol. Struct.* 1207, 127750.
- Balasubramanian, P., Murugakoothan, R., Jayavel, 2010. Synthesis, growth and characterization of organic nonlinear optical bis-glycine maleate (BGM) single crystals. *J. Cryst. Growth.* 312, 1855–1859.
- Deepa, B., Philominathan, P., 2017. Enhanced NLO and antibacterial properties of nicotinic acid-doped KDP crystals: synthesis, growth and characterisation. *Mater. Res. Innov.* 21, 86–90.
- Shen, Guang-Zhi, Zou, Gui-Hua, Li, Hai-Yan, Zou, Yu-Long, 2019. Crystal structure and antibacterial activity of polyoxometalate cobalt-ciprofloxacin complex. *J. Mol. Struct.* 1198, 126831.
- Raval, Hiral, Parekh, B.B., Parikh, K.D., Joshi, M.J., 2019. Growth and Characterizations of Organic NLO Imidazolium L-Tartrate (IMLT) Single Crystal. *Adv Cond Matter Phys.* 2019, 1–9.
- Helen, F., Kanchana, G., 2014. Growth and characterization of metal ions doped L-serine NLO single crystals for optoelectronic applications. *Optik.* 125 (9), 2051–2056.
- Kandhan, S., Tamil Arasan, B., Krishnan, P., Aravindhan, S., Srinivasan, S., Gunasekaran, S., 2019. Structural, optical and piezoelectric investigation on brucinium bromide hydrate nonlinear optical single crystal for optical parametric oscillators, high-power laser, piezo-sensors and transducers applications. *J. Mol. Struct.* 1180, 512–522.
- Kandhan, S., Krishnan, P., Jagan, S., Srinivasan, R., Gunasekaran, S., 2018. Structural, optical and piezoelectric investigation on new Brucinium Chlorate di-hydrate NLO single crystal for optoelectronic, piezo-sensor, transducer and OLED applications. *Opt. Mater.* 84, 556–563.
- Karuppasamy, P., Pandian, Muthu Senthil, Ramasamy, P., 2017. Crystal growth and characterization of third order nonlinear optical piperazinium bis (4-hydroxybenzenesulphonate) (P4HBS) single crystal. *J. Cryst. Growth.* 473, 39–54.
- Kui, Wu., Yang, Zhihua, Pan, Shilie, 2017. A first quaternary diamond-like semiconductor with 10-membered LiS41 rings exhibiting excellent nonlinear optical performances. *CHEM COMMUN.* 21, 3010–3013.
- Kalaivani, D., Arthi, D., Mukunthan, A., Jayaraman, D., Joseph, V., 2015. Growth and characterization of L-lysine succinate single crystal. *J. Cryst. Growth.* 426, 135–140.
- Kurtz, S.K., Perry, T.T., 1968. A powder technique for the evaluation of nonlinear optical materials. *J. Appl. Phys.* 39, 3798–3813.
- Zhang, Liming, Yan, Pengchao, Li, Yan, He, Xihong, Dai, Yujie, Tan, Zhilei, 2020. Preparation and antibacterial activity of a cellulose-based Schiff base derived from dialdehyde cellulose and L-lysine. *Ind Crops Prod.* 145, 112126.
- Min-hua jiang., Qi Fang., 1999. Organic and semiorganic Nonlinear Optical Materials. *Adv. Mater.* 11, 1147–1151.
- Ozga, K., Krishnakumar, V., Kityk, I.V., Jasik-Słezak, J., 2008. L-lysine monohydrochloride dihydrate as novel elasto- and electrooptical materials. *Mater. Lett.* 62, 4597–4600.
- Prakasha, P., Gnanaprakasama, P., Emmanuela, R., Arokiyarajb, S., Saravananc, M., 2013. Green synthesis of silver nanoparticles from leaf extract of *Mimusops elengi*, Linn. for enhanced antibacterial activity against multi drug resistant clinical isolates. *Colloid Surf. B.* 108, 255–259.
- Pasupathi, G., Philominathan, P., 2008. Investigation on growth and characterization of a new inorganic NLO material: Zinc sulphate (ZnSO₄:7H₂O) doped with Magnesium Sulphate (MgSO₄:7H₂O). *J. Mater. Sci.* 62, 4386–4388.
- Ravathi, V., Karthik, K., 2019. Physico-chemical properties and antibacterial activity of Hexakis (Thiocarbamide) Nickel (II) nitrate single crystal. *Chem. Data Collect.* 21, 100229.
- Rathika, A., Ganapathi Raman, R., 2014. Investigations on growth and characterisation of 2-hydroxyanilinium 3, 5-dinitrobenzoate single crystal. *Mater. Res. Innov.* 19, 182–186.
- Ramesh Babu, R., Vijayan, N., Gopalakrishnan, R., Ramasamy, P., 2006. Growth and Characterisation of L-Lysine monohydrochloride dehydrate (L-LMHCL) single crystal. *Cryst Res Technol.* 41, 405–410.
- Shanmuga Sundaram, M., Vijayalakshmi, V., Dhanasekaran, P., Balasundaram, O.N., Palaniswamy, S., 2019. Growth and characterization of L-alanine potassium nitrate single crystals for nonlinear optical applications. *J. Cryst. Growth.* 506, 122–126.
- Sivavishnu, D., Srineevasan, R., Johnson, J., 2018. Synthesis, growth, optical, band gap and mechanical properties of semiorganic nonlinear optical material: 2-Aminopyridine potassium dihydrogen orthophosphate lithium chloride (2APKDPL) crystal. *Mater. Sci. Energy Technolog.* 1, 205–214.
- Tauc, J., 1974. Amorphous and liquid semiconductors. Plenum, Newyork.
- Ushasree, P.M., Jayavel, R., Subramaniyan Ramasamy, P.J., 1999. Growth of zinc thiourea sulfate (ZTS) single crystals: a potential semiorganic NLO material. *J. Cryst. Growth.* 197, 216–220.
- Vasudevan, V., Ramesh Babu, R., Bhagavannarayana, G., Ramamurthi, K., 2010. Effect of metal and aminoacid dopants on the growth and properties of L-lysine monohydrochloride dehydrate single crystal. *Mater Chem Phys.* 124, 681–688.
- Zou, Yu-Long, Lia, Hai-Yan, Zhoua, Wei, Cuib, Xin-Gang, Zouc, Gui-Hua, Shenc, Guang-Zhi, 2020. Introduction of the antibacterial drugs Norfloxacin and Ciprofloxacin into a polyoxometalate structure: Synthesis, characterization, and antibacterial activity. *J. Mol. Struct.* 1205, 127584.